

INFORMATION TO USERS

This manuscript has been reproduced from the microfilm master. UMI films the text directly from the original or copy submitted. Thus, some thesis and dissertation copies are in typewriter face, while others may be from any type of computer printer.

The quality of this reproduction is dependent upon the quality of the copy submitted. Broken or indistinct print, colored or poor quality illustrations and photographs, print bleedthrough, substandard margins, and improper alignment can adversely affect reproduction.

In the unlikely event that the author did not send UMI a complete manuscript and there are missing pages, these will be noted. Also, if unauthorized copyright material had to be removed, a note will indicate the deletion.

Oversize materials (e.g., maps, drawings, charts) are reproduced by sectioning the original, beginning at the upper left-hand corner and continuing from left to right in equal sections with small overlaps. Each original is also photographed in one exposure and is included in reduced form at the back of the book.

Photographs included in the original manuscript have been reproduced xerographically in this copy. Higher quality 6" x 9" black and white photographic prints are available for any photographs or illustrations appearing in this copy for an additional charge. Contact UMI directly to order.

UMI[®]

Bell & Howell Information and Learning
300 North Zeeb Road, Ann Arbor, MI 48106-1346 USA
800-521-0600

SYNTHESIS OF MAGNETIC NANOPARTICLES USING REVERSE MICELLES

A Dissertation

**Submitted to the Graduate Faculty of the
University of New Orleans
In partial fulfillment of the
requirements for the Degree of**

**Doctor Of Philosophy
in
The Department of Chemistry**

By

Everett E. Carpenter

B.S., Appalachian State University, 1994

August 1999

UMI Number: 9946675

**Copyright 1999 by
Carpenter, Everett E.**

All rights reserved.

**UMI Microform 9946675
Copyright 1999, by UMI Company. All rights reserved.**

**This microform edition is protected against unauthorized
copying under Title 17, United States Code.**

UMI
300 North Zeeb Road
Ann Arbor, MI 48103

Copyright 1999, Everett E. Carpenter


DOCTORAL DISSERTATION REPORT

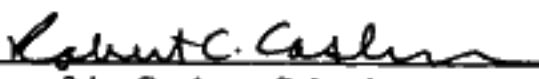
Candidate: Everett E. Carpenter

Major Field: Chemistry

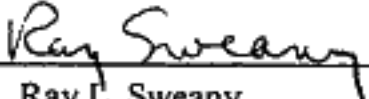
Title of Dissertation: Synthesis of Magnetic Nanoparticles
Using Reverse Micelles

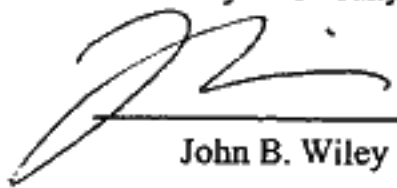
Approved:



Major Professor & Chair
Charles J. O'Connor


Dean of the Graduate School
Robert C. Cashner

EXAMINING COMMITTEE:


Ray L. Sweany


John B. Wiley


Bruce C. Gibb


Scott L. Whittenburg

Date of Examination:

June 22, 1999

ACKNOWLEDGEMENT

“For me chemistry represented an indefinite cloud of future potentialities which enveloped my life to come in black volutes torn by fiery flashes, like those which had hidden Mount Sinai. Like Moses, from that cloud I expected my law, the principle of order in me, around me, and in the world. . . . I would watch the buds swell in spring, the mica glint in the granite, my own hands, and I would say to myself: “I will understand this, too, I will understand everything.”” Primo Levi (1919–87), Italian chemist, author. *The Periodic Table*, “Hydrogen”

I would like to thank my family and friends for their support and understanding while I pursue my chemistry.

TABLE OF CONTENTS

ACKNOWLEDGEMENT.....	iii
TABLE OF CONTENTS.....	iv
LIST OF FIGURES.....	vii
LIST OF TABLES.....	ix
ABSTRACT.....	x
CHAPTER 1, INTRODUCTION.....	1
1.1 Preface.....	1
1.2 Synthesis Methods.....	2
1.2.1 Introduction.....	2
1.2.2 Surfactants.....	3
1.2.3 Micelles.....	4
1.3 Characterization.....	20
1.3.1 Transmission Electron Microscopy.....	20
1.3.2 Energy Dispersive Spectroscopy.....	21
1.3.3 Structure Types.....	21
1.3.4 X-ray diffraction.....	27
1.3.5 Extended X-ray Absorption Fine Structure.....	30
1.3.6 Magnetic Characterization.....	31
CHAPTER 2, METAL AND ALLOY MATERIALS.....	51
2.1 Abstract.....	51
2.2 Introduction.....	51
2.3 Experimental Section.....	52

2.4 Results and Discussion.....	53
2.5 Conclusion.....	64
CHAPTER 3, ANTIFERROMAGNETIC MATERIALS	66
3.1 Abstract	66
3.2 Introduction	66
3.3 Experimental	68
3.4 Results and Discussion.....	69
3.5 Conclusion.....	84
CHAPTER 4, FERRIMAGNETIC MATERIALS	85
4.1 Abstract	85
4.2 Magnetic Properties of a Series of Ferrite Nanoparticles.....	86
4.2.1 Introduction	86
4.2.2 Experimental Section	86
4.2.3 Results And Discussion.....	87
4.3 Atomic Structure of MnFe_2O_4 Nanoparticles.....	97
4.3.1 Introduction	97
4.3.2 Experimental	97
4.3.3 Magnetic Characterization	98
4.3.4 EXAFS Studies	102
4.3.5 Discussion	108
4.4 Conclusion.....	109
CHAPTER 5, NANOCOMPOSITE MATERIALS.....	111
5.1 Abstract	111

5.2 Synthesis of Gold-Coated Iron Nanoparticles.....	112
5.2.1 Introduction	112
5.2.2 Experimental	113
5.2.3 Characterization	114
5.2.4 Core-Shell Discussion	122
5.3 Synthesis Au-Fe-Au Nano-Onion Structures.....	124
5.3.1 Motivation	124
5.3.2. Experimental	128
5.3.3 Characterization	131
5.3.4 Magnetic Measurements.....	141
5.3.5 Electronic Measurements	144
5.3.6 Conclusion.....	147
Chapter 6, CONCLUSION.....	148
References	150
VITA	159

LIST OF FIGURES

Figure 1.1. Schematic phase diagram of a surfactant-oil-water system.....	5
Figure 1.2. Chemical Representation of two surfactants used in the following chapters. .	8
Figure 1.3. Model of the location of solutes in reverse micelles.....	12
Figure 1.4. Size distribution histogram of monodispersed palladium particles synthesized in reverse micelles.	18
Figure 1.5. The hexagonal, cubic, and body-center packing structures.	23
Figure 1.6. Pervoskite structure of KMnF_3	25
Figure 1.7. Spinel Structure.....	28
Figure 1.8. Magnetic ions can order ferromagnetically, antiferromagnetically, ferrimagnetically, or canted antiferromagnetically,	34
Figure 1.9. Plot of size effect on coercivity.	36
Figure 1.10. Representative spin state energy diagram.....	38
Figure 1.11. Magnetic ions can couple in three fashions: direct coupling, superexchange, and indirect coupling.	41
Figure 1.12. Thermal variations in magnetic susceptibility of $\gamma\text{-Fe}_2\text{O}_3$	47
Figure 2.1. TEM micrograph of CoPt alloy nanoparticles.....	54
Figure 2.2. Typical XRD powder pattern of gold coated CoPt_3	57
Figure 2.3. A DC susceptibility plot of gold coated CoPt.....	60
Figure 2.4. A magnetization versus field plot of gold coated CoPt_3 alloy at 2 K.	62
Figure 3.1. TEM micrograph of 35 nm KMnF_3	70
Figure 3.2. Size histogram and TEM of spherical 22 nm KMnF_3	72

Figure 3.3. Experimental and simulated X-ray powder diffraction patterns of 22 nm sample.....	74
Figure 3.4. ZFC and FC magnetic susceptibility of 13 nm KMnF_3 sample.....	78
Figure 3.5. Hysteresis loop at 4.5 K of the 22 nm KMnF_3 sample.....	81
Figure 4.1. Susceptibility as a function of temperature for 5 nm Fe_3O_4 nanoparticles. ..	89
Figure 4.2. Magnetization versus field for 5 nm Fe_3O_4 particles.....	92
Figure 4.3. TEM micrograph of 5 nm Fe_3O_4 particles.....	95
Figure 4.4. Susceptibility as a function of temperature for sample I of MnFe_2O_4	100
Figure 4.5. Mn EXAFS data of samples S1, S2 and S3.....	104
Figure 4.6. Mn EXAFS data of samples S2, S5 and S6.....	106
Figure 5.1. A typical powder diffraction pattern of iron-gold core shell nanocomposites.	115
Figure 5.2. TEM image of 12 nm iron-gold core-shell.....	117
Figure 5.3. FC and ZFC susceptibility of 12 nm iron-gold core-shell.....	119
Figure 5.4. Schematic representation of gold/iron/gold Nano-Onion structure.....	126
Figure 5.5. A representation of the sequential synthesis scheme.....	129
Figure 5.6. A representative energy dispersive spectra (EDAX) of Au/Fe/Au nano-onion.	132
Figure 5.7. A representative XRD pattern of Au/Fe/Au nano-onion.....	135
Figure 5.8. Selected area microdiffraction pattern of Au/Fe/Au nano-onion.....	137
Figure 5.9. Representative micrograph of Au/Fe/Au nano-onion.....	139
Figure 5.10. Magnetic susceptibility versus temperature of Au/Fe/Au nano-onion.....	142
Figure 5.11. Resistance versus temperature of Au/Fe/Au nano-onion.....	145

LIST OF TABLES

Table 2.1. Summary of magnetic data obtained on four different metal and alloy samples.	59
Table 3.1. Structural and magnetic properties of a series of KMnF_3 samples.	77
Table 4.1. Magnetic Properties of ferrite nanoparticles.	88
Table 4.2. Summary of reaction conditions for the synthesis of MnFe_2O_4	99
Table 5.1. Magnetic properties of iron/gold core-shell nanocomposites.	123

ABSTRACT

Nanoparticles are single crystallites or composite materials in which the dimensions are within 1 to 100 nm in scale. Synthesizing nanoparticles with very narrow size distribution and high uniformity is one of the prime goals of this research. To achieve the high uniformity aqueous reactions are carried out using the confined aqueous core of a reverse micelle can be used as a “nano-reactor”, thus allowing us to carry on aqueous reactions, such as precipitation reactions, within a confined space and gaining the advantage of size restriction.

We present the magnetic properties of eight different nanoparticles synthesized within reverse micelles. The particles are separated into four chapters depending on their magnetic properties and structure. In chapter one we present the synthesis and magnetic properties of cobalt platinum alloys. These alloys are superparamagnetic and display higher coercivities than cobalt particles of the same size. Alloying displays one method of improving the coercivity of metal nanoparticles.

The synthesis of the antiferromagnetic KMnF_3 is presented in chapter two. The synthesis of KMnF_3 nanoparticles using reverse micelles is presented for the first time. The particles display a highly uniform cubic structure. The particles display an antiferromagnetic ordering temperature of 88 K and a blocking temperature which varies with particle size between 36 and 10 K.

Aqueous reactions allow for a greater variation of reaction conditions. In chapter three the manganese ferrite nanoparticles synthesized in reverse micelles is presented for the first time. 5 nm MnFe_2O_4 are superparamagnetic with a blocking temperature of 33 K. For comparison two other common ferrites, Fe_3O_4 and CoFe_2O_4 , were also

synthesized. Reaction conditions demonstrated an effect on the overall cation distribution between the A and B sublattice of the spinel. This redistribution did not have a pronounced affect on magnetic properties.

Lastly, a sequential synthesis is presented where iron and gold are grown in core-shell and "nano-onion" like structures. These particles have the favorable magnetic properties of iron while remaining protected from oxidation by a gold shell. The effect of the gold shell on the magnetic properties of coercivity and blocking temperature is discussed. Although the thickness of the gold shell is varied between 2 and 3 nm, there is not a change in the coercivity or blocking temperature within experimental error. In addition, the electronic properties of the "nano-onions" were studied. Gold-Iron-Gold nano-onions display a -1.5% magnetoresistance. The particles undergo a transition from itinerate to localized electrons resulting in a 400% increase in resistance as the particles are cooled to 10 K.

CHAPTER 1, INTRODUCTION

1.1 Preface

Nanoparticles are materials that have grain sizes less than 100 nanometers. Interest in nanoparticles has grown over the past two decades due to changes in the physical, electronic, magnetic, and optical properties resulting from the small grain size. As the size of the particles is reduced, much of the bulk-grain behavior changes to resemble atomic size regimes. It is this change in bulk-properties which has fueled an explosive growth in nanophase research. Magnetic materials that have nanoscale dimensions are of particular interest.

Magnetic nanoparticles have a wide range of applications. One of the most aggressively pursued areas is in high-density magnetic memory. Areal density in longitudinal magnetic recording has surpassed the 1 Gbit/in² level and continues to grow at an impressive rate each year. Current media are composed of CoPtCr alloys due to the low noise and high coercivity. In order to push the areal density even higher, it is important to engineer magnetic materials which have a higher intrinsic coercivity while maintaining low intergrain exchange coupling.¹

Soft magnetic ferrites, such as Fe₃O₄ and Fe₂O₃, offer many advantages in radio frequency applications where the complex permeability can be modified by external fields or by changing the composition. The flexibility offered during the synthesis of ferrites allows for versatility in applications as rf filters. The radio noise characteristics of the ferrite filters made from nanocrystalline alloy materials are superior due to their increased attenuation range.²

Nanophase magnetic materials have many applications outside those of the telecommunications and computer industries. Magnetic materials with a grain size less than 100 nm can be stabilized as ferrofluids. Ferrofluids are magnetic colloid solutions that are used everywhere from high-end consumer speakers to gas valve sealing and lubrication. The ferrofluids are held in place by a large magnetic field, thereby gaining the advantages of both contact and hydrodynamic seals.³

It was this vast range of applications for magnetic nanoparticles that prompted the lofty goal of achieving improved magnetic properties using nanoparticles. With this in mind, attention was turned toward determining which synthesis method would help reach this goal. Hopefully along the way, a greater understanding of the magnetic properties of nanoparticles could be attained.

1.2 Synthesis Methods

1.2.1 Introduction

Many of the advantages of nanoparticles are enhanced by narrow size distributions and uniform morphology. For example, in the case of magnetic memory, the noise level between grain boundaries is increased with high levels of dispersion in sizes. There are many different synthesis methods for magnetic nanoparticles. In general, the synthesis techniques can be broken down into two categories, physical and chemical methods. In physical methods, a bulk precursor is physically broken down into smaller grain sizes. In chemical methods, the particles are synthesized via chemical reactions in nanophase dimensions.⁴

There are several different physical methods for preparing nanoparticles, such as attrition⁵, sputtering⁶, and ablation.⁷ Mechanical attrition, such as ball milling, is a non-equilibrium process that can produce a wide range of alloys and composites which cannot be prepared in conventional methods. Sputtering and ablation both rely on the evaporation of a target and subsequent condensation on the substrate. In sputtering the evaporation is achieved using an electric arc while ablation relies on a high energy laser to evaporate the target. Both sputtering and ablation can be adapted to generate a variety of metals, oxides, or salts. Physical methods have a high degree of versatility; however they typically do not generate highly uniform nanoparticles.

A wide variety of chemical methods have been used to synthesize nanoparticles such as precipitation⁸, reduction⁹, pyrolysis¹⁰, and hydrothermal reactions.¹¹ In precipitation and reduction methods, the nanoparticles are synthesized by rapid chemical reaction and quenched to limit or prevent crystallization. In pyrolysis, volatile organometallics, like $\text{Fe}(\text{CO})_5$, are used and the ligands removed by thermal decomposition to yield the nanoparticles. In hydrothermal synthesis, aqueous reactions are carried out at elevated temperatures and pressures. Since the early 1980's, a growing area of chemical synthesis involved surfactants.¹²

1.2.2 Surfactants

Surfactants get their name from the acronym "surface acting agent". They are used to help affect the surface tension along interfaces. Surfactant molecules contain a long chain hydrocarbon plus a hydrophilic end. Typically the hydrophilic end group comes in the form of an ionic group, such as a sulfate or quaternary amine, forming either anionic or cationic surfactants, respectively. Nonionic surfactants having either ethers or

alcohol functional groups are also common. This combination of polar and non-polar groups allows the surfactant to help solubilize water within an organic medium.¹³

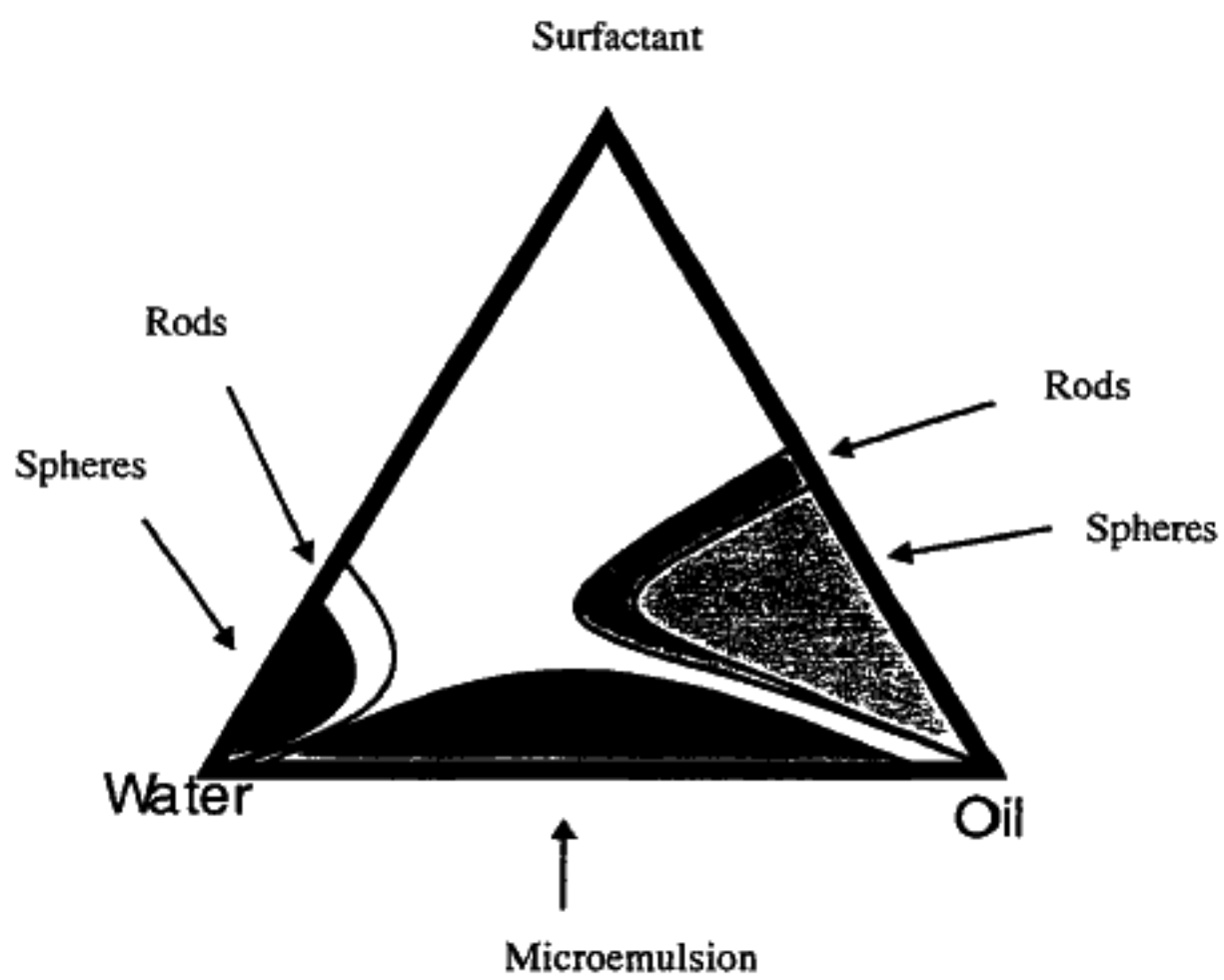
One interesting phenomenon in a water-oil-surfactant system is the presence of self-assembled arrays of surfactants called micelles. In 1963, Winsor noted that certain mixtures of oil, water, and surfactant yielded a clear, seemingly one-phase system.¹⁴ This system, called a micelle or microemulsion solution, contained small droplets of one liquid dispersed within the other with a self-assembled layer of surfactant molecules along the interface between the phases. The self-assembly is driven by thermodynamic factors to minimize surface tensions.¹⁵ Micelle solutions were originally characterized with a bulk aqueous phase where the hydrophobic carbon chains were turned inward to help stabilize the oil phase. Later, reverse micelles were also characterized where the conditions were reversed.¹³ A bulk oil phase was used with the hydrophilic head groups turned inward to help stabilize the water phase. A representative three component phase diagram is presented in Figure 1.1.

Micelles exist in very specific conditions dictated by the molar ratio of oil, water, and surfactant. However, the formation of micelle solutions is driven by the differences in the polarity of the two groups; any factor which affects the polarity such as temperature, co-surfactants, or salt concentration also affect the stability of the micelle solution. If the ratio of water to surfactant concentration changes greatly the micelle solution becomes unstable forming a traditional emulsion solution.

1.2.3 Micelles

When surfactants are dissolved in organic solvents they form spherical aggregates called reverse micelles. Micelles can be formed both in the presence and absence of

Figure 1.1. Schematic phase diagram of a surfactant-oil-water system. The areas nearest the lower corners are regions which are characterized by spherical micelles, moving out from there are regions of rod-like microemulsions. The lower region between water and oil is a characteristic macroemulsion region



water, however in the absence of water they are very small. When water is added, it is readily solubilized into the polar area of the micelle forming a water pool. This water pool is characterized by ω , the molar water to surfactant ratio ($\omega = [\text{H}_2\text{O}]/[\text{S}]$). Typically aggregates containing a small amount of water (below $\omega=15$) are usually called reverse micelles while microemulsions correspond to droplets containing large amounts of water molecules.¹⁶ This distinction between micelle and microemulsion is often times blurred and the two terms are used interchangeably.¹⁵

The spherical nature of the surfactant aggregates in reverse micelles is a response to a thermodynamically driven process. It basically represents a need for the surfactants to reach an energetically favorable packing configuration at the interface depending on the molecular geometry of the surfactant.¹⁷ The surfactant molecules can be represented as a truncated cone whose dimensions are determined by the hydrophilic and hydrophobic parts of the surfactant. This geometry is presented in Figure 1.2.

Assuming water-in-oil droplets are spherical, the radius of the sphere is expressed as:

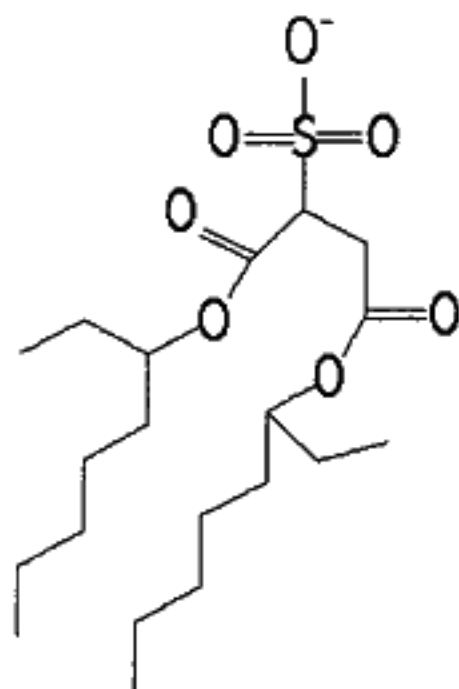
$$R=3V/\Sigma$$

where, R is the radius, V is the volume, and Σ is the surface area. Assuming that the water molecules govern the volume and the surfactant molecules determine the surface area then the water pool radius can be expressed as:

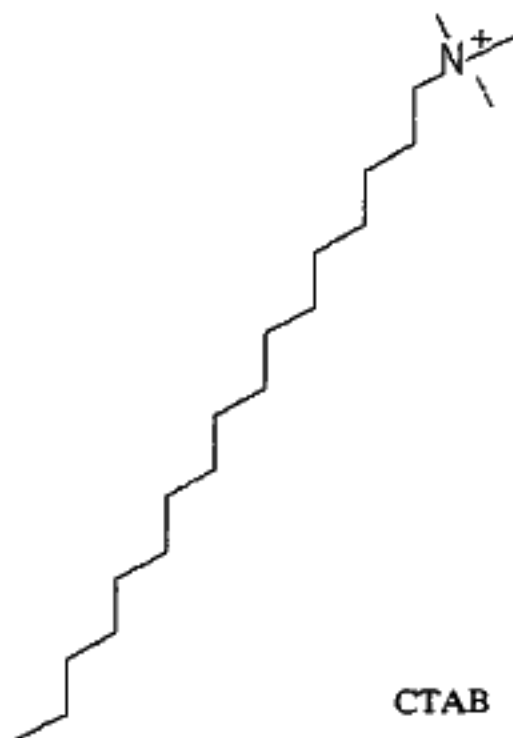
$$R_w=3V_{aq}[\text{H}_2\text{O}]/\sigma[\text{S}]$$

where R_w is the radius of the water pool, V_{aq} is the volume of water molecules and σ is the area per polar head group of surfactant.

Figure 1.2. Chemical Representation of two surfactants used in the following chapters.
AOT (dioctylsulfosuccinate sodium salt) and CTAB (cetyltrimethylammonium bromide).



AOT



CTAB